DOI: 10.13009/EUCASS2023-510
Aerospace Europe Conference 2023 – 10TH EUCASS – 9TH CEAS

Further Progress in Aerodynamic Studies for CALLISTO - Reusable VTVL Launcher First Stage Demonstrator

Josef Klevanski[1], Bodo Reimann[2], Sven Krummen[3], Moritz Ertl[4], Tobias Ecker[5], Johannes Riehmer[6]
Etienne Dumont[7], Lâle Evrim Briese[8] and Thiemo Matthias Kier[9]

[1]DLR, Institute of Aerodynamics and Flow Technology, Supersonic and Hypersonic Technologies Department, Linder Hoehe, 51147 Cologne, Germany, Josef.Klevanski@dlr.de

[2]DLR, Institute of Aerodynamics and Flow Technology, Spacecraft Department, Lilienthalplatz 7, 38108, Braunschweig, Germany, Bodo.Reimann@dlr.de

[3]DLR, Institute of Space Systems, Robert Hooke-Str. 7, 28359 Bremen, Germany, Sven.Krummen@dlr.de

[4]DLR, Institute of Aerodynamics and Flow Technology, Spacecraft Department, Bunsenstr. 10, 37073 Gottingen, Germany, Moritz.Ertl@dlr.de

[5]DLR, Institute of Aerodynamics and Flow Technology, Spacecraft Department, Bunsenstr. 10, 37073 Gottingen, Germany, Tobias.Ecker@dlr.de

[6]DLR, Institute of Aerodynamics and Flow Technology, Supersonic and Hypersonic Technologies Department, Linder Hoehe, 51147 Cologne, Germany, Johannes.Riehmer@dlr.de

[7]DLR, Institute of Space Systems, Robert Hooke-Str. 7, 28359 Bremen, Germany, Etienne.Dumont@dlr.de

[8]DLR, Institute of System Dynamics and Control, Department of Space System Dynamics, 82234 Weßling, Germany, Lale.Briese@dlr.de

[9]DLR, Institute of System Dynamics and Control, Department of Aircraft System Dynamics, 82234 Weßling, Germany, Thiemo.Kier@dlr.de

Abstract

DLR, CNES and JAXA jointly continue the developing of a vertical take-off and landing (VTVL) reusable subscaled first stage demonstrator CALLISTO, which has to show the capability to launch, land and relaunch a vehicle under conditions representative for the first stage of an operational launch vehicle in the several demo-flights. Furthermore, during CALLISTO demonstration flights, data will be gathered to improve knowledge on the operation of a reusable vehicle which will help to optimize the reusability capabilities of future launch systems [1-2]. The key challenge is to create an extensive aerodynamic data base covering all the flight configurations and conditions. Indeed, the aerodynamic performance plays a central role in the global performance of CALLISTO. In the period of 2020-2022 the extensive aerodynamic database (AEDB) with uncertainties and aerothermodynamic database (ATDB) based on the numerous CFD-simulations and wind tunnel measurement campaigns were created. The actual AEDB and ATDB relate to the detailed layout of CALLISTO corresponding to the state of 2019-2020 called aeroshape CAL1C. At the same time, in the process of design development, significant changes and details were made to the layout of the demonstrator, resulting in a new aerodynamic shape called CAL1D (state 2022). The limited computing resources and time plan do not allow repeating all CFD-simulations and wind tunnel test campaigns performed for CAL1C. The paper will discuss the concept and methodology called "delta-aerodynamics" for the ongoing work which allows applying the existing database for the new aeroshape CAL1D with minor corrections.

1. Introduction

The pursuit of reusable space launch vehicles has become a key challenge in recent years. The main motives for introducing reusability are twofold: reducing the costs associated with access to space and increasing the operational flexibility of launch systems. In addition, reusability can improve the reliability of space launches and solve the problem of recycling used launch vehicle stages. In this regard, extensive research projects and studies have been conducted to study the reuse of launch vehicle components. The pioneering achievements made by companies like

DOI: 10.13009/EUCASS2023-510

SpaceX and Blue Origin in reusing elements of space transportation systems based on the vertical takeoff and vertical landing (VTVL) concept have injected renewed momentum into this area of exploration. In order to remain competitive in the international launch market, the Japan Aerospace Exploration Agency (JAXA), Centre National d'Études Spatiales (CNES) of France, and the German Aerospace Center (DLR) have forged a close partnership to develop, construct, and fly the experimental reusable VTVL demonstrator named CALLISTO (Cooperative Action Leading to Launcher Innovation in Stage Toss-back Operations) [1], [2], [7] and [8]. CALLISTO serves as a flight demonstrator for future reusable launcher stages and their associated technologies. This collaborative program aims to enhance their capabilities throughout the project. These capabilities encompass various aspects, such as product and vehicle design, establishment of the ground segment, and post-flight operations for vehicle recovery and reuse. The primary objective is to demonstrate the ability to recover and reuse a vehicle under conditions representative of a future operational launcher. This research project provides a unique opportunity to develop, refine, and test the critical technologies and knowledge required for the successful implementation of reusability. Several test and demonstration flights are planned for CALLISTO, enabling the accumulation of invaluable experience in the recovery and reuse of a vehicle.

CALLISTO will perform several test- and demo-flights to demonstrate the capability to recover and reuse a vehicle under conditions representative of a future operational launcher and to gather the related experience.
Following a successful Preliminary Design Review (PDR), the project has transitioned into the detailed design phase for the launch system and its sub-systems [11]. As part of the extended aerodynamic studies, numerous outputs have been identified to meet the project's requirements. These outputs include the estimation of global and local aerodynamic coefficients, assessment of distributed aerodynamic loads, evaluation of the impact of thrust throttling and plume deflection on aerodynamic characteristics, and definition of critical flight conditions.

- Estimation of the global aerodynamic coefficients CX, CY, CZ, CMx, CMy, CMz for the 6-DoF flight dynamics simulation and for the development of the GNC-System.
- Estimation of the local aerodynamic coefficients for structural load estimation and aerodynamic shape optimization.
- Estimation of the distributed aerodynamic loads: dCX/dX, dCY/dX, dCMZ/dX etc for structural load estimation.
- Evaluation of the thrust throttling impact on the aerodynamic characteristics.
- Evaluation of the plume deflection impact by Thrust Vector on the aerodynamic characteristics.
- Definition of the critical flight conditions

The main objectives are:

- Creation of the 6-Dof AErodynamic Data Base (AEDB) containing the aerodynamic function for the calculation of the forces and moments for all configurations, including estimated uncertainties
- Creation of the Aero-Thermodynamic Data Base (ATDB) containing the aerothermodynamic function for the calculation of the thermal loads for all configurations, including estimated uncertainties

The AEDB should also provide a continuous solution for the transition modes between the so-called base configurations. Therefore, special studies of the thrust throttling impact and of the thrust deflection impact on the aerodynamic were also performed and diverse transition functions were developed.

The intensive aerodynamic studies were continued in 2022-2023.

2. Mission analysis and flight configurations

Using only one engine for a demonstration vehicle is a very challenging task, since an acceptable thrust-to-weight ratio for both launch and landing must be achieved. This is much more difficult compared to launch vehicles with multiple rocket engines, like the Falcon 9 with 9 engines. The available engine thrust with a minimum throttle ratio limits the launch mass as well as the landing mass.

According to various constraints and limitations, the dynamic pressure along the trajectory is relatively high – in some cases too high to perform a tilt-over and boost-back manoeuvre relying on RCS (reaction and control system) thrusters only. As an alternative, the boost-back manoeuvre can be performed by deflection of the main engine with TVC while the engine is still running.

The primary mission objective is to demonstrate a so-called "toss-back" flight profile, which includes in particular the following phases:

DOI: 10.13009/EUCASS2023-510

- classic ascent phase (when compared to an expendable launch vehicle)
- attitude change phase, with tilt-over manoeuvre
- boost-back phase with targeting the landing site
- aerodynamic guided descent phase
- final landing boost and touchdown ("pin-point" landing)

A candidate trajectory is shown in Figure 1. As an additional option, performing an ascent phase with the deployed, actively controlled fins is considered.

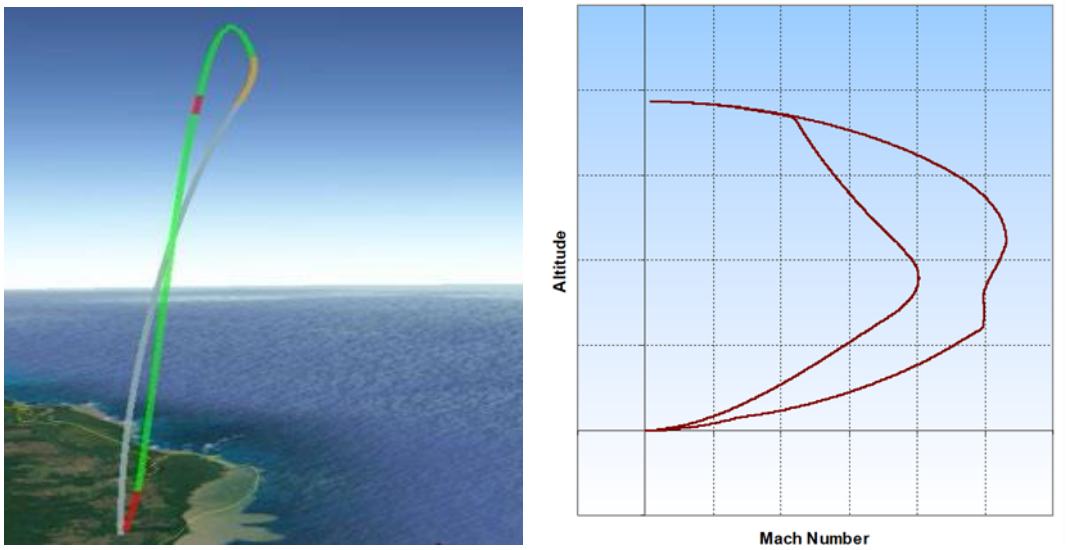

Figure 1: Candidate trajectory.

The nomenclature of the main flight configurations used in accordance with the demo flight phases (Configurations FFO – UUN) and the nomenclature of the additional flight configurations used for the test flights and for the transition between configurations is given in Table 1. Note that aerodynamic characteristics of the vehicle on the launch pad before launch is also the object of CFD computations (not presented here) and may influence the design of the CALLISTO system.

Table 1: CALLISTO flight configurations.

CONF	FFO	FFN	UFN	UFO	UUO	UUN	FUFN	FUFO	FUUO	FUO
Picture										
Flight Phase	Ascent: MEIG#1 ↓ MECO#1	Ballistic: MECO#1 ↓ Fin Depl.	Ballistic & Aerodyn. Descent: Fin Depl. ↓ MEIG#2	Brake & Approach Boost: MEIG#2 ↓ Legs Deploy	Landing: Legs Depl. ↓ MECO#2 (Touch-down)	Landed (Park): After MECO#2	Transition: FFN ↓ UFN	Transition: FFO ↓ UFO	Transition: FUO ↓ UUO	Test Flights A, B
Fins	Folded	Folded	Unfolded	Unfolded	Unfolded	Unfolded	F→U	F→U	F→U	Folded
Land. Legs	Folded	Folded	Folded	Folded	Unfolded	Unfolded	Folded	Folded	Unfolded	Unfolded
Thrust Plume	Yes	No	No	Yes	Yes	No	No	Yes	Yes	Yes

DOI: 10.13009/EUCASS2023-510

In fact, on top of the reference flight profile, several flight profiles are under investigation in order to establish a consistent flight test plan which would enable the incremental increase of the difficulty of the flight up to the reference flight profile. Before the demo-flight this extensive incremental program of test flights is to be performed and therefore many additional configurations are also be analysed. The planned flight classes and the corresponding aerodynamic configurations are shown in Table 2:

Table 2: planned flight and corresponding aerodynamic configurations.

Flight Class	Configurations
Test Flight A	FUO
Test Flight B	FUO → UUO
Test Flight C	FFO → UFO → UUO
Test Flight D	FFO → FFN → UFN → UFO → UUO
Test Flight E (DEMO)	FFO → FFN → UFN → UFO → UUO
Test Flight E (Option)	UFO_ASC → UFN → UFO → UUO

Thus, the aerodynamic database of CALLISTO is very extensive: Mach number, altitude and dynamic pressure vary in a very broad range; the vehicle flies forwards in the ascent phase and rearwards in the approach and landing phases, during the tilt-over manoeuvre the angle of attack varies from 0 to 180°. Furthermore, the flight configuration changes for each flight phase: the aerodynamic control surfaces (fins) and landing legs are stowed during the ascent phase, the fins are then deployed for the aerodynamic descent phase. Finally, the landing legs are deployed shortly before the touch-down.
The trajectory was analysed to indicate the flight phases and configurations which are particularly important from an aerodynamic perspective. For each flight phase and configuration, the relative forces were compared: aerodynamic forces, thrust and RCS-forces. It can be seen that from aerodynamic point of view, the most important phase is the aerodynamically controlled descent, or in other words the flight configuration UFN.
The configuration FFN is not as critical as in this case the vehicle weight is largely dominating, but it shows the limitation of the RCS capabilities.
Both configurations UFN and UFO requires knowledge of the whole range of AoA = 0° to +180°.
In the case of FFO configuration, knowledge of aerodynamic characteristics and especially the drag is important for small angles of attack (AoA), in the range: -5° to +5°. For the FFN configuration in the culmination point the flight direction changes to the opposite, so the AoA varies in the range of AoA = 0° to +180°.

3. AEDB Extension for Test Flight C

During 2020-2022, an AEDB for all CALLISTO configurations, which allows 6DoF flight dynamics simulations first of all, the reference mission, has been largely created. However, the detailed analysis of the planned test flights showed that in order to simulate some of the test flights, especially, the Test flight C, the AEDB needed an extension: During the Test Flight C the flight direction of CALLISTO changes from the flight forwards to the flight rearwards in FFO-configuration with deep throttling of the engine thrust without its complete shutdown and the hovering under impact of the side is also probable. Especially for the simulation of this test flight, the aerodynamic database of the FFO configuration for small Mach Numbers, previously prepared for use in the range of angles of attack from 0° to 40°, was extended for use in the range of angles of attack from 0° to 180°, considering deep thrust throttling. The database extensions designated as FFO_40_GLO and FFO_100_GLO cover 6DoF-simulation of the Test Flight C for this case.

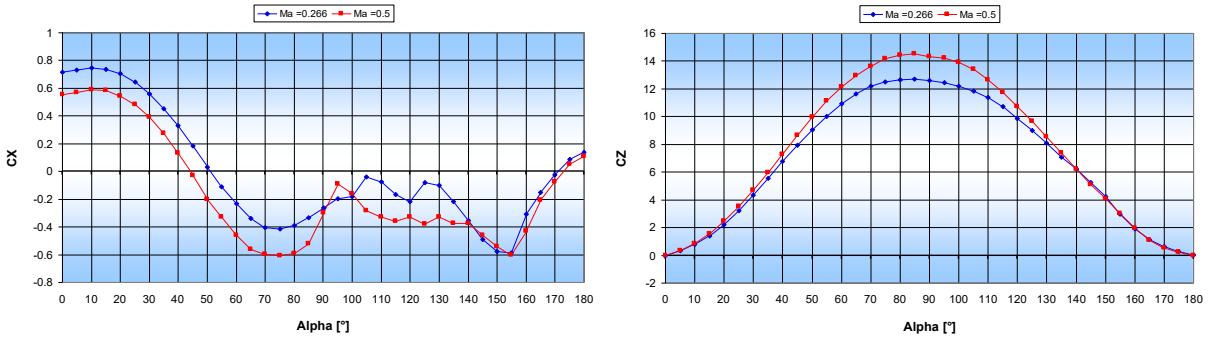

Figure 2: CX, CZ = f(AoA) FFO, Thrust = 40%.

DOI: 10.13009/EUCASS2023-510

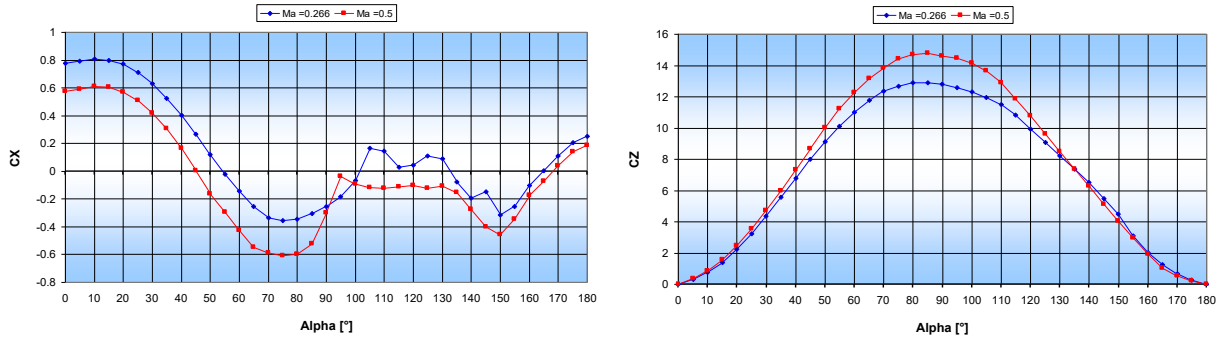

Figure 3: CX, CZ = f(AoA) FFO_GLO, Thrust = 100%.

In addition, specifically to simulate the transient mode like fins deployment the AEDB was additionally extended for the so called FUFN configuration (FFN->UFN).
Three database extensions are prepared (Transition-Configurations for Fin Deployment):

- FUFN_GLO (FFN → UFN)
- FUFO_40_GLO (FFO → UFO)
- FUUO_40_GLO (FUO → UUO).

For trajectory accuracy of the 6DoF-Simulation of the Demo-Flights use of the databases FUFN_GLO, FUFO_40_GLO is not critical: The Fin Deployment for the Demo-Flight should be performed in high altitude with small velocity and very small dynamic pressure and will have practically no effect on the trajectory. These databases could rather be used for the simulation of the actual unfolding process (especially the local coefficients). The Database FUFO_40_GLO can also efficiently be used for Test Flight C simulation:

- Test flight C: FFO → UFO → UUO

The Database FUUO_40_GLO is well suited for the simulation of Test Flight B:

- Test flight B: FUO → UUO

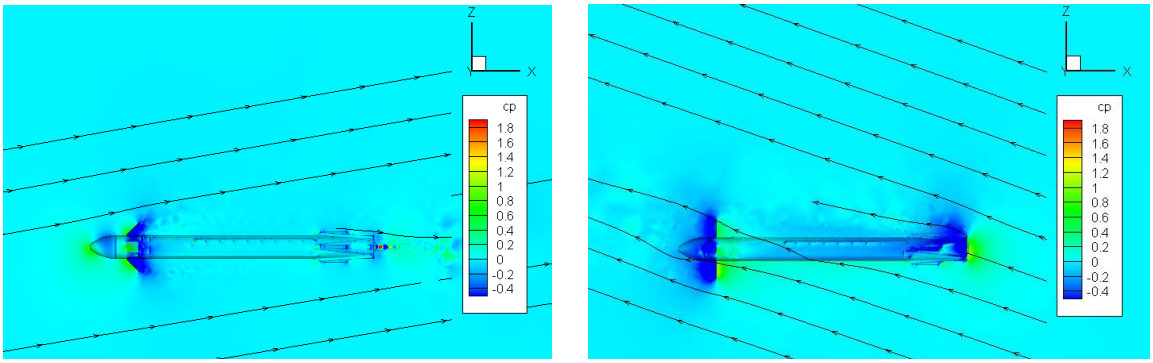

Figure 4: Fins-Deployment (Configurations: FUFO and FUFN).

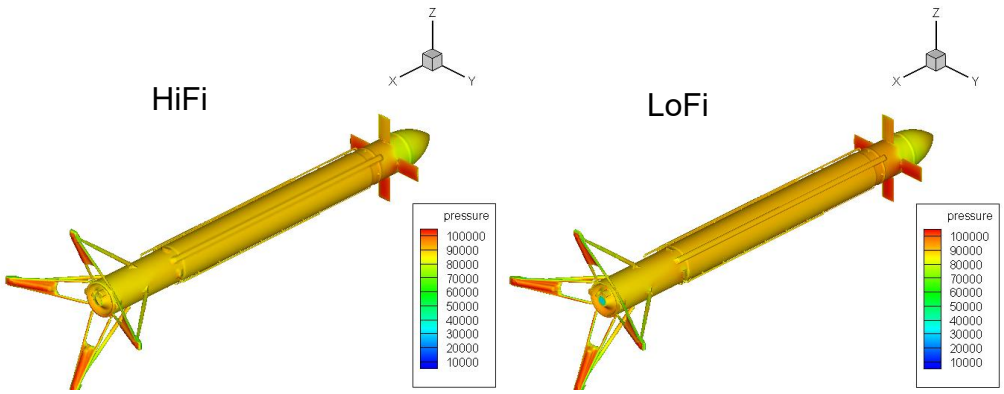

Figure 5: Fins-Deployment (FUUO Validation).

DOI: 10.13009/EUCASS2023-510

However, the transition from the FUUO with fins unfolded 90° to the configuration with normal working position of fins (UUO Deflection -10°...0°...+10°) can be done via the interpolation. These data sets can be used to simulate 6DoF flight dynamics without any angle of attack and roll constraints: They are the spherical polars.

4. Models Adequacy and Uncertainties. "Delta-Aerodynamics" Concept

The adequacy of any model to the real object cannot be absolute – it is always not perfect: No model can fully reflect all properties and features of the object in all aspects. Any model contains numerous assumptions and simplifications, both conscious and involuntary, as well as various inaccuracies.

In principle, the differences between the characteristics of a real-world object (CALLISTO itself) and its model should be covered by the so-called uncertainties. Such uncertainties can be of a different nature, for example: They can be both inaccuracies in the CFD methods used to calculate aerodynamic characteristics, measurement errors in the WTT campaigns, or deliberately introduced simplifications into the model. Expected uncertainties, their statistical interpretation and the way they are applied in Monte Carlo simulations are an important component of the created aerodynamic database.

The actual AEDB and ATDB relate to the detailed layout of CALLISTO corresponding to the state of 2019-2020 called aeroshape CAL1C. At the same time, in the process of further design development, significant changes and details were made to the layout of the demonstrator (Chapter 6), resulting in a new aerodynamic shape called CAL1D in 2022.

To consider uncertainties of the computed aerodynamic loads with respect to the CFD RANS solver two turbulence models have been investigated. Figure 6 shows results for drag and pitching moment for the CAL1C UFN configuration flying backwards with engine off. The coefficients have been simulated with of two different turbulence models, a Spalart-Allmaras (SA) and a Reynold stress model (RSM). The RSM shows a significant higher drag for all relevant Mach numbers (left), the pitching moment versus angle of attack (right) shows smaller values compared to the SA model. These variations have to be covered by the uncertainties in the final AEDB. Also shown in Fig.7 are the data of the current AEDB.

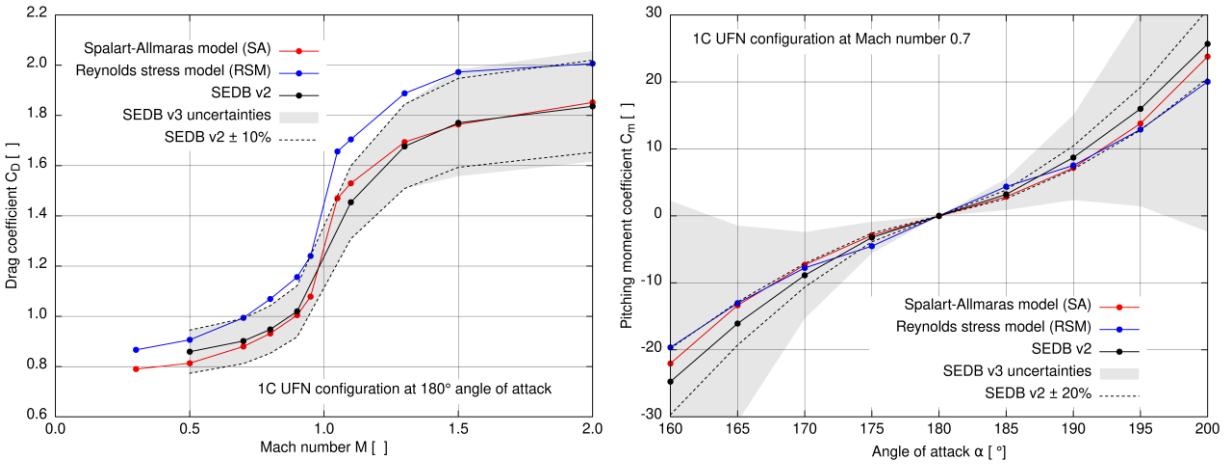

Figure 6: Influence of the turbulence model on drag and pitching moment coefficient for the 1C UFN configuration.

Under the conditions of limited computing resources and a very intensive and tight time plan, it is not possible to repeat all the necessary CFD calculations and wind tunnel tests, performed earlier for CAL1C-shape, in full.
Therefore, the concept and methodology called "**delta-aerodynamics**" was proposed to apply the existing database for the new aeroshape CAL1D with only minimal necessary corrections.

An updated "watertight" aerodynamic shape has been prepared, considering almost all the detailed changes made to the layout of the demonstrator as results of the further development during 2021-2022. For all configurations of this aerodynamic shape, designated CAL1D, meshes were generated for CFD calculations, for both Low Fidelity and High Fidelity. The meshes characteristics are given in Table 3.

DOI: 10.13009/EUCASS2023-510

Table 3: Mesh-Characteristics CAL1C vs. CAL1Ds.

Configuration	CAL1C LoFi	CAL1D LoFi	CAL1C HiFi	CAL1D HiFi
FFN	~2.7 Mln. Elem.	~5.9 Mln. Elem.	~100 Mln. Elem.	~120 Mln. Elem.
FFO	~2.7 Mln. Elem.	~5.9 Mln. Elem.	~78 Mln. Elem	~154 Mln. Elem.
UFN	~2.9 Mln. Elem.	~6.0 Mln. Elem.	~123.3 Mln. Elem.	~147.7 Mln. Elem.
UFO	~2.9 Mln. Elem.	~6.3 Mln. Elem.	~65 Mln. Elem.	~167 Mln. Elem.
UFO_ASC	~2.9 Mln. Elem.	~6.3 Mln. Elem.	~65 Mln. Elem.	~161 Mln. Elem.
UUO	~3.5 Mln. Elem.	~6.5 Mln. Elem.	~23 Mln. Elem.	~86 Mln. Elem.

A list of control design cases (Table 4) was compiled, in tight accordance with CNES, which included all typical flight modes for all configurations, considering both test and demonstration trajectories. For all these check cases, aerodynamic control CFD calculations were performed both for the aerodynamic form CAL1C, which was the basis for the existing database AEDB, and for the new aerodynamic shape CAL1D.

Table 4: Flight Points for Delta Aerodynamics

H	M	AoA	AoR	Fins	Thrust	Configuration
7100	0.7	0	0	0	110%	UFO
8600	0.8	0	0	0	110%	UFO
7100	0.9	180	0	0	0	UFN
7100	0.9	180	0	0	20%, 40%, 110%	UFO
5000	0.8	180	0	0	110%	UFO
0	0.2355	180	0	0	40%	UUO
7100	0.9	175	45	0/0/0/0	0	UFN
7100	0.7	5	0	0	110%	FFO
8600	0.8	5	0	0	110%	FFO
7100	0.9	170	0	0	0	UFN
5000	0.8	175	0	0	110%	UFO
7100	0.9	175	45	+5/-5/-5/+5	0	UFN
0	0.2355	155	0	0	40%	UUO

After comparison with the existing AEDB created for CAL1C the further actions should be performed (listed according to its priority):

1. If the differences in the total coefficients are relative small (inside of the uncertainties): Use of the existing AEDB also for the new aeroshape CAL1D will be allowed.

2. If the differences in the total coefficients are bigger (slightly outside of the uncertainties): The uncertainties in the existing AEDB should be increased.

3. If the differences in the total coefficients are huge (significantly outside of the uncertainties): The relevant data in AEDB should be corrected.

In the following sections, some features of the demonstrator that are not directly included in the mathematical model, but significantly affect the model accuracy and uncertainties, are discussed in more detail, and first of all, the impact of change in the aerodynamic shape (Chapter 6) and the effect of elastic deformation of the stabilizers on their efficiency (Chapter 7).

5. Classical and Bayesian Estimation of Uncertainties in AEDB

As presented in previous chapter, a precise characterisation of the aerodynamic properties of the CALLISTO vehicle before its maiden flight is not possible. Moreover, all results from experimental and computational studies of the aeroshape are approximating the real-world behaviour of the final flight vehicle. The quality of approximation and the individual error characteristics are depending on the applied methodology, the dynamic and geometric similarity to the flight configuration, and the achievable precision of measurement or simulation. Therefore, to reduce the systematic impact of such errors, extensive CFD simulations with various degrees of fidelity for the shape and mesh (see Chapter 4) and WTT experiments in different wind tunnels and setups [6] have been conducted to estimate the nominal aerodynamic properties of CALLISTO by mutual comparison. This diversified approach can be considered as state-of-the-are for the nominal aerodynamic characterisation of aerospace vehicles [9].

DOI: 10.13009/EUCASS2023-510

For RLVs however, not only the estimation of the nominal aerodynamic properties but also a quantification of uncertainty in those estimates is essential for successful development: Since the vehicle has to perform a precise landing at the end of flight, the mission profile and the Guidance, Navigation and Control (GNC) system needs to be designed robustly against perturbations and uncertainties [10]. Depending on the applied methodologies, these down-stream development tasks require an uncertainty quantification either in terms of probability distributions or in terms of confidence intervals on the nominal estimates.
In contrast to the estimation of the nominal aerodynamic properties, the estimation of the associated uncertainties is rather complex and difficult, since the dataset cannot be arbitrarily extended due to costs and practical constraints, and the assessment and integration of expert knowledge in an uncertainties model is very labour-intense. Therefore, two different approaches have been followed for CALLISTO: A “Classical Approach”, which is mostly based on manual expert assessment and heritage, and a “Bayesian Approach”, which is still experimental but may be performed in an automated way [11].

For the Classical Approach, a model of the nominal aerodynamic coefficients is generated by low degree polynomial interpolation of an (ideally) coherent subset of the AEDB. Then, the remaining datapoints are used to specify expected error bars around the nominal model by expert assessment, which are mostly constant or proportional to the nominal value. If a probabilistic uncertainty model is required, these error intervals can further be used as confidence intervals for simple probability distributions. Particularly for CALLISTO, the nominal model has been generated by piece-wise linear interpolation of the CAL1C LoFi CFD dataset, while the remaining CFD and WTT datasets have been examined to specify constant and proportional error boundaries for the uncertainties model, which shall be used as 3-sigma levels for a normal distributed error. An excerpt of this classical model is visualized in the left graph in Figure 7. The main advantage of this classical approach is the relatively simple mathematical structure of the fitted model, which supports good understanding of the error terms. Therefore, it eases the incorporation of heritage and expert knowledge, while it simultaneously reduces the risk of overfitting. Also, high-performant computer implementations are possible for the prediction of disturbed aerodynamic coefficients due to this simple structure. The main disadvantage of this approach is the manual assessment and fitting process for the error terms. This requires a lot of human workforce and make the model inherently subjective. Also, complex error contributors are difficult to identify and consider in this process, while frequent updates of the model are not feasible.

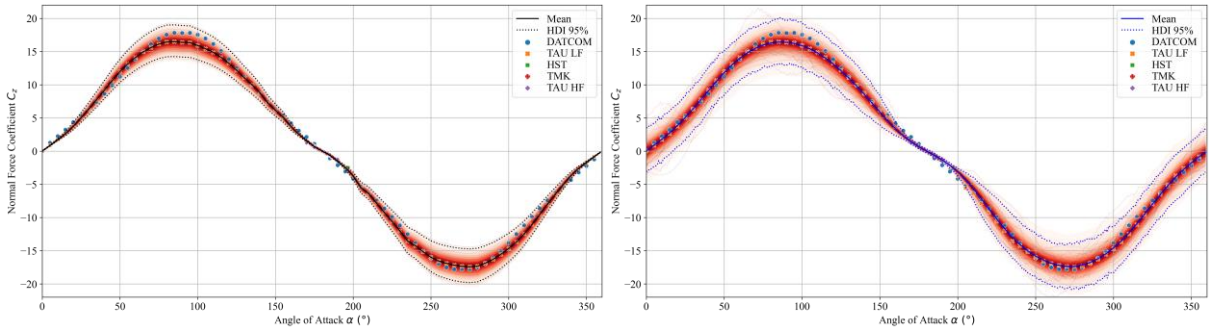

Figure 7: Probability density of the predicted uncertainties in the AEDB dataset for UFN configuration with Ma=0.5 and φ=0°. Left: Classical model manually fitted by expert’s assessment; Right: Bayesian model automatically fitted by inference of posterior probability via MCMC sampling.

For the Bayesian Approach, on the other hand, a Bayesian network is used to specify a probability distribution over the aerodynamic coefficients in dependence of latent probabilistic parameters. This probability distribution is fitted simultaneously to all available datapoints by inference of the posterior distribution over the parameter space, using computational approximation techniques such as Markov Chain Monte Carlo (MCMC) sampling. Based on this fitted model, the posterior predictive distribution over the aerodynamic coefficients can be computed. Particularly for CALLISTO, a Gaussian Process model has been defined, implemented and fitted via the software package PyMC [12], as visualized in the right graph Figure 7. Other models have also been specified and are currently under further investigation. The main advantage of this approach is the fully automated fitting process, which allows the consideration of complex models and error contributors, as well as allows frequent re-fitting as soon as new data arrives. This reduces the required expert’s workforce significantly. The main disadvantage is however the complex mathematical structure of the model, which makes this incorporation of heritage and expert knowledge more difficult, and also increases the computational requirements for model fitting and prediction.

DOI: 10.13009/EUCASS2023-510

An exemplary comparison of the classical with the Bayesian model is shown in Figure 7. It can be seen that the datasets of the normal force coefficient in dependency of the angle of attach is globally fitted quite well. Furthermore, it can be observed that uncertainty levels are reduced in both models around $\alpha \approx 160°...200°$, which is caused by the higher data point density in this region from WTT or CFD HiFi datasets. More detailed analyses [11] revealed, that the quality of fit, expressed as root mean square error or median absolute deviation, is very similar for both models, giving no clear evidence to identify a better model. However, it could be observed that the classical model has higher bias to the datapoints, whereas the Bayesian model possesses a larger variance.
Currently, further refinements of the Bayesian uncertainties model are undertaken to model more characteristics of the aerodynamic database of CALLISTO. Also, other Bayesian models are investigated and tested as alternative to the presented Gaussian Process model. The goal is to create a complete but suitable Bayesian characterization of CALLISTO's AEDB and to mature the Bayesian Approach for the development of future launch vehicles. For the ongoing development of the CALLISTO vehicle, the classical model will still be used as baseline, due to the higher heritage on this process, whereas the Bayesian models will mostly be used for model comparison and amendments.

6. CALLISTO Shape Evolution

In the preliminary design phase numerous vehicle layouts have been considered and analysed. The development of the CALLISTO aerodynamic shape was accomplished with intensive aerodynamic studies: each layout was checked by extensive CFD simulations.
Whereas in the initial development phase of CALLISTO the aerodynamic team defined the aerodynamic shape of the vehicle (CAL1B in Figure 8) and the structure designers had to realise it, in this phase of detailed development the aerodynamic a new task was given to the aerodynamic team: to assess the effect of the numerous design details on the aerodynamic performance compared to the ideal shape and to reduce the negative effects wherever possible.
The aerodynamic shape of the vehicle has become considerably more complex as a result of the further development of the design: numerous "superstructures" and protuberances such as cable ducts and external pipelines have appeared, the vehicle became not symmetric anymore.

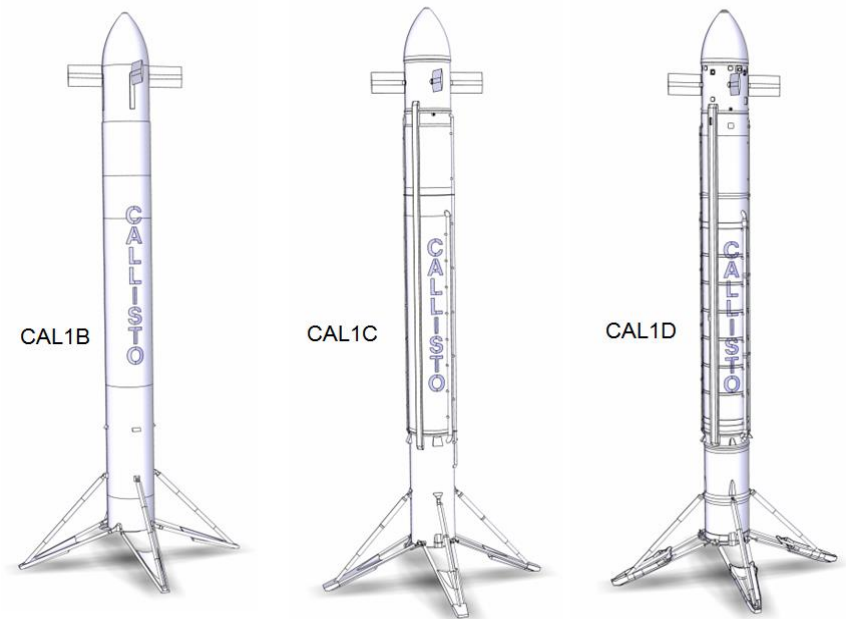

Figure 8: Aerodynamic shapes CAL1B, CAL1C and CAL1D.

The aerodynamic shape, which considered these additional design details, was finally defined in 2020 and designated as shape CAL1C (Figure 8). This shape became the basis for both the so-called "watertight shape" and further mesh generation for CFD calculations [2] (LoFi as well as HiFi), and for the manufacturing of aerodynamic models for the wind tunnels measurements campaigns [6] in TMK (2020, model scale 1:35) and in HST (2020, model scale 1:10).
In particular, on the basis of this aerodynamic form CAL1C the aerodynamic database AEDB and aerothermodynamic database ATDB were created in 2020-2021.

However, the design development of the demonstrator did not stop and the corresponding changes in the layout continued to be made.

DOI: 10.13009/EUCASS2023-510

One of the first challenges was the assessment for the local aerodynamics: The structure design implied by the use of the so-called L-flanges for the reliable and easy connections for vehicle section. But the impact of the uncovered L-flanges led to very significant increase of the aerodynamic drag. The measures proposed by the aerodynamics team were the use of inclined ramps to improve the flow around the flanges. This local optimization has significantly reduced the negative effect of the L-Flanges.

In particular, the design of external pipelines, their outer diameter, considering the thermal insulation, connection points and fastenings to the demonstrator body, have been changed. The size and shape of the cable channels have also been changed. The geometry of special cavities for the nozzles of the reactive control system RCS on the equipment bay EVB was determined. One of the most significant differences was the change in the shape of the aerodynamic covers of the landing legs, as well as the change in the kinematics of their opening, which, in turn, changed the angle of contact of the legs to the body in the folded position. This change significantly affected the aerodynamic drag, as can be seen in Figure 9.

This actual aerodynamic shape, which finally was defined in 2022, received the designation CAL1D (Figure 8)

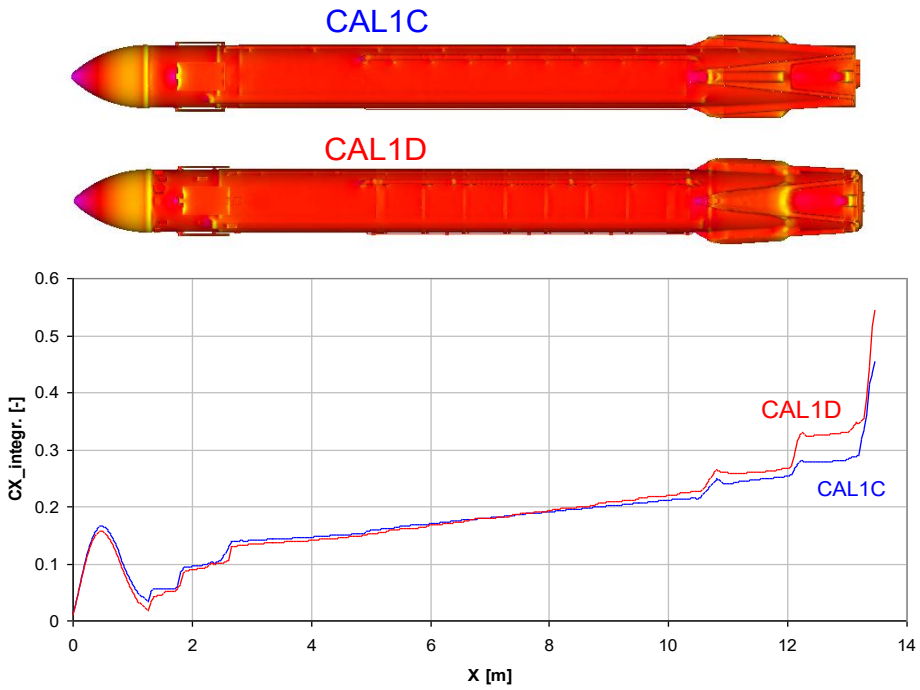

Figure 9: Impact of the Aeroshape evolution on the drag (FFO-Configuration).

7. Deformation Impact on the Fin Efficiency

Structural elastic deformation of the aerodynamic control surfaces resulting from aerodynamic loads along the flight trajectory may have a significant impact on the fin efficiency. In particular, due to deformation of the aerodynamic control surfaces caused by aerodynamic loads during flight, the fin effectiveness can change considerably leading to a potential deviation between commanded, measured, and effective deflection angles. Including the actuator stiffness and additional flexibilities due to the attachment of the fins to the vehicle structure, this aeroservoelastic interaction is not represented by the AEDB which is derived based on a reference configuration of the vehicle without structural elastic effects or additional flexibilities due to the actuator interfaces. Therefore, these unmodeled effects have to be reflected within the uncertainties and subsequently applied onto the AEDB results.

In CALLISTO, specific technical requirements of the vehicle cover these effects by defining boundaries regarding the acceptable deformation of the aerodynamic control surfaces. In this context, the influence of the fin deformation has to be assessed for pre-defined mechanical load cases under representative environmental conditions while considering the actuator influence and for specific deformation patterns. In particular, the deformation patterns shall cover bending deformation in lift and drag direction, as well as torsional deformation as indicated in Figure 10. Since the applied

DOI: 10.13009/EUCASS2023-510

methods in this section do not account for in-plane deformations in drag direction, this case will not be discussed further in this paper. Furthermore, the critical load cases in the technical requirements are represented by a combination of high Mach numbers with high effective angles of attacks which can be obtained from the total angle of attack of the vehicle in combination with the deflection angle of the corresponding aerodynamic control surfaces. However, these pre-defined critical load cases are significantly beyond nominal load cases covered by CALLISTO's reference trajectory for the final demonstration flights. While the full assessment of the deformation impact on the fin efficiency extended well beyond the expected flight envelope to account for the aforementioned critical load cases, only the results along the reference trajectory will be presented in this paper.

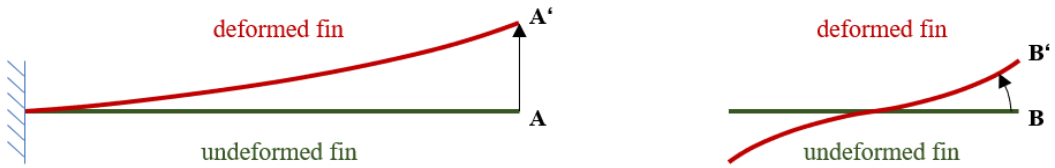

Figure 10: Schematic overview of the aerosurface bending and torsional deformation.

In contrast to high-fidelity fluid-structure interaction studies which often require not only increased computational effort and time, but also adaptive meshing between the structural and aerodynamics models represented by Global Finite Element (GFEM) and Computational Fluid Dynamics (CFD) models, the studies in this paper were performed by low-fidelity numerical methods with the MATLAB-based tool VARLOADS [17]. Although VARLOADS is most commonly used for typical aircraft configurations as described in [18]-[20], it has been applied in CALLISTO for dynamic stability studies of the aerodynamic control surfaces within a pre-defined flight envelope to assess the likelihood for flutter [21]. However, the vehicle structure is these studies is neglected and only the aerodynamic control surfaces in conjunction with the actuator stiffness and flexible attachment to the vehicle structure remain, resulting in a model configuration similar to an experimental wind-tunnel setup with a flexible hinge. This particular modeling approach is also used in this paper to obtain the aeroservoelastic deformation of the aerodynamic control surfaces along the reference flight trajectory as indicated in Figure 11.

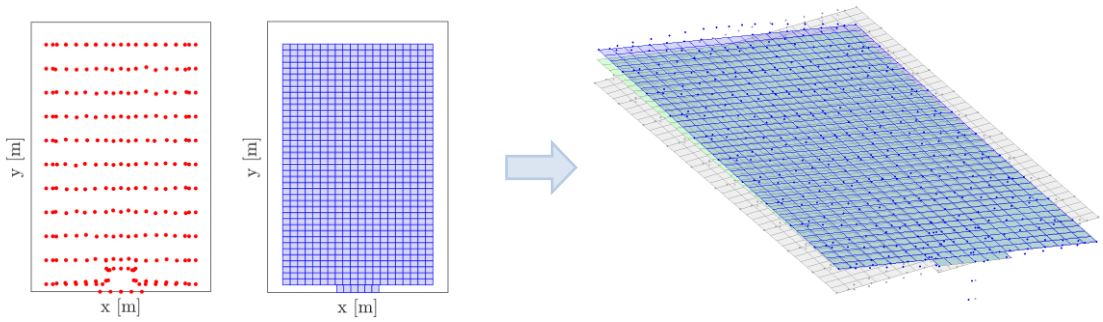

Figure 11: Condensed structural dynamic model (red) and aerodynamics panel model (blue) on the left and splined aeroservoelastic model on the right representing the total deformation for Mach = 0.9 and δ=10deg

The condensed structural dynamic model is obtained by Guyan reduction from an integrated Finite Element model of the aerodynamic control surface with almost 700.000 degrees of freedom, resulting in a model with round about 435 uniformly distributed boundary nodes as indicated in Figure 11. To account for additional flexibilities, the structural dynamic model is extended beforehand by the actuator stiffness matrix as well as the interface stiffness matrix of the vehicle equipment bay (VEB) which is the cylindrical core structure at which the actuators and fins are attached to. For load-dependent entries of the actuator stiffness matrix only the worst-case values are used, while the off-diagonal elements of the non-symmetric stiffness matrix are assumed to be negligible. It is important to notice, that only small deformations are considered in the subsequent studies such that the linear elastic theory remains valid, and that the mass-normalized mode shapes are available from a modal analysis with fixed boundary conditions.

In contrast to the dynamic stability studies in [21], where the Doublet Lattice Method (DLM) was used to compute frequency-dependent Aerodynamic Influence Coefficient (AIC) matrices for the unsteady aerodynamics, the Vortex

DOI: 10.13009/EUCASS2023-510

Lattice Method (VLM) is applied to obtain the steady aerodynamic matrices. Similar to the DLM, the VLM allows for fast computation of the steady aerodynamic matrices for lifting surfaces based on potential equations neglecting viscous effects. Due to these inherent simplifications, several physical features of the aerodynamic flow such as boundary layer effects, turbulence, flow separation, shocks induced by local supersonic flow, or thickness effects cannot be captured by the VLM. For the aeroservoelastic studies, the aerodynamic control surface is modelled as a two-dimensional planar lifting surface with approximately 1000 uniformly distributed panels. In accordance with the experimental wind-tunnel setup mentioned previously, a symmetry condition is applied at the origin of the reference aerodynamic coordinate system (y=0m). More information on the underlying modeling approach regarding the condensed structural dynamics and the aerodynamics panel model can be found in [21].

The coupling between the structural and aerodynamics models is further realized by using Infinite Plate Splines (IPS) based on Radial Basis Functions (RBF). The generalized aerodynamic forces and deflections can then be obtained and mapped back onto the structural grid by applying the equations provided in [18]-[21]. The total deformation of the aerodynamic control surface is finally computed by a superposition of the rigid deflection of the structure by the effective angle of attack δ with the actual deformation of the structure due to the applied aerodynamic loads. This approach is depicted in Figure 11 on the right by the reference configuration in grey, the rigid deflection of the structure in green, as well as the total deformation of the aerodynamic control surface due to a coupling between the aerodynamic loads and the structural elastic properties in blue. As indicated in Figure 10, the necessary information to assess the technical requirements can then be easily obtained by extracting the local translational and rotational deformation of the structural nodes at the fin tip.

The aerodynamic loads obtained by the VLM were compared with CFD results for CAL1C regarding the spanwise lift distribution on the aerodynamic control surface at dedicated flight conditions as shown in Figure 12. Even though the magnitude and shape of the lift distributions at different flight conditions are comparable, it is important to notice that the low- and high-fidelity CFD results are obtained for a configuration where the complete vehicle structure is included in the computation as shown in the previous chapters, while the low-fidelity numerical investigations using VLM are only performed for the aerodynamic control surfaces neglecting the vehicle structure. Therefore, potential perturbations and interactions between the vehicle structure and the aerodynamic control surfaces cannot be well-represented. This is also showcased by the deviation from the quasi-elliptical lift distribution especially in the low-fidelity CFD results. Furthermore, an increase in lift contribution at the fin tip is depicted for both CFD results which could be caused by turbulent flow along the fin tip edge which in turn cannot be detected by the aerodynamic panel approach. In general, for higher effective angle of attacks, the low-fidelity numerical investigations tend to be more conservative mainly due to the linear extrapolation of the aerodynamic loads based on the effective angle of attack.

Finally, the bending and torsional deformations of the fin along the reference flight trajectory were assessed while excluding flight regimes where the aerodynamic control surfaces are not deployed as well as flight regimes above Mach = 0.95 due to the validity boundaries of the VLM and altitudes higher than 15 km which are not covered by the underlying atmosphere model. For the remaining flight trajectory, the impact of torsional deformation on the fin efficiency is displayed in Figure 13, where the dashed lines in the left plot indicate the acceptable deviation from the commanded fin deflection including the torsional deformation as defined in the corresponding uncertainty model. This shows that under nominal flight conditions along the reference trajectory, the fin efficiency remains well-below the pre-defined uncertainty boundaries within the validity of the applied methods. Additionally, on the right plot, the torsional deformation along the flight trajectory is presented with respect to the effective angle of attack acting on the aerodynamic control surfaces showcasing the differences between positive and negative effective angles of attack at higher and lower altitudes and corresponding Mach numbers. This shows similar to the left plot that along the flight trajectory the torsional deformation remains below ±1deg in accordance with the technical requirements regarding the acceptable deformation limits of the aerodynamic control surfaces.

Based on the results presented in this section, future studies will address the impact of the vehicle structure on the fin deflection by performing dynamic response studies incorporating the actuator dynamics. Furthermore, by comparing systematically the CFD results with low-fidelity VLM results, the VLM database will be updated allowing a more accurate representation of the aerodynamic loads and corresponding fin deformations.

DOI: 10.13009/EUCASS2023-510

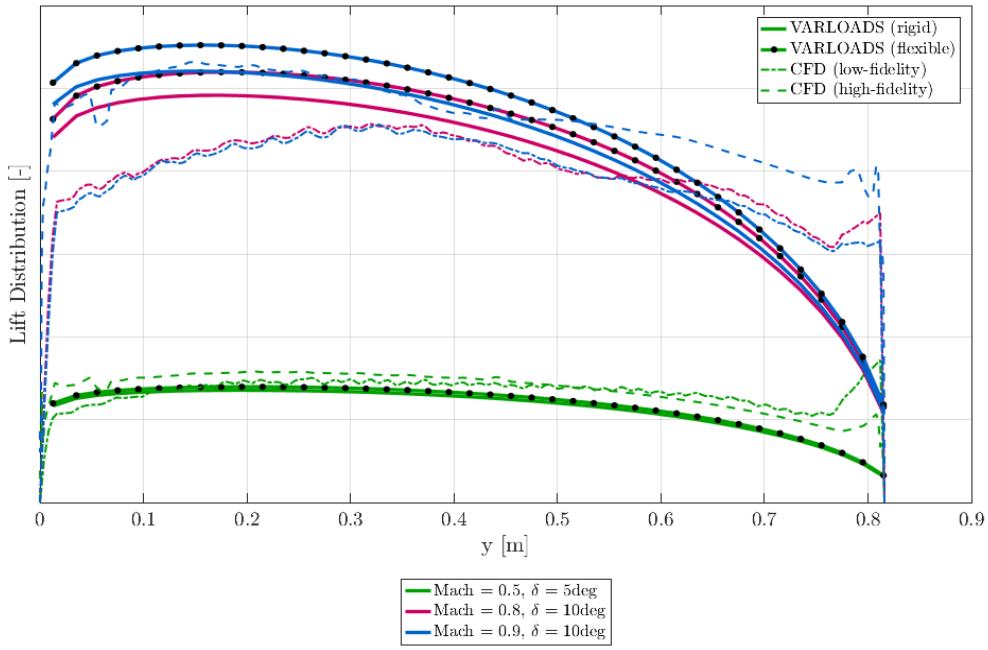

Figure 12: Comparison of spanwise lift distributions on the aerodynamic control surface at dedicated flight conditions (different Mach numbers and effective angle of attacks)

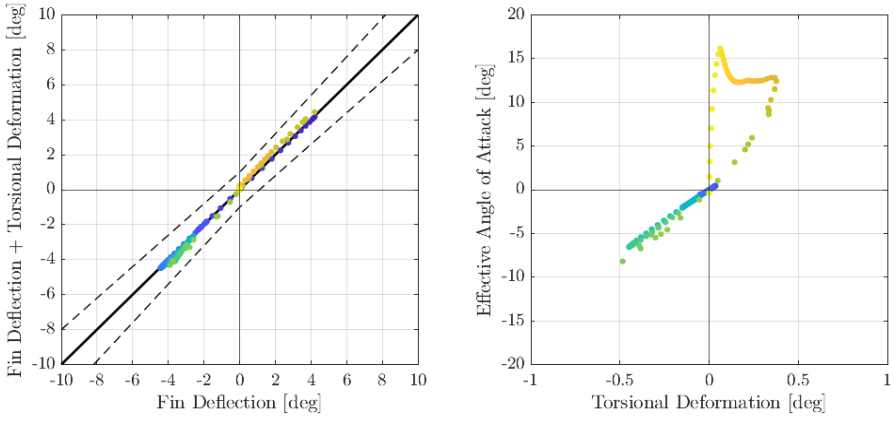

Figure 13: Deformation impact on the fin deflection for uncertainty computations

8. Aerothermodynamic Aspects

Aerothermal loads as well as mechanical loads, are determining factors in the design during launcher development as the thermal loads impact thermal protection system during product design and trajectory optimisation. For the purpose of characterizing the aerothermal properties and loads of the CALLISTO vehicle aerothermal databases are generated periodically based on current aeroshape and flight domain. Due to the collaborative nature of the CALLISTO design process loads definition and respective thermal interfaces (tanks, landing legs, etc.) for the entire vehicle are defined. While the CAL1B aeroshape had 15 thermal interfaces, the number of interfaces for the CAL1C aeroshape has increased to more than 50 thermal interfaces due to is detailed description involving no symmetry and many of the final mechanical extensions (cable ducts, pipes, etc.). Compared to previous databases for the CAL1B shape, the extended aerothermal database for the CAL1C was tripled to nearby 200 2D CFD calculations and more than 40 High-Fidelity 3D CFD while the number of grid points increased equally. The final updated aerothermal database, based on the CAL1C-aeroshape but applicable for the actual CAL1D-aeroshape, allows interpolation of interface heatfluxes for

DOI: 10.13009/EUCASS2023-510

the entire flight domain at varying angle of attack (between 180° and 160°). More details can be found in references [3] and [4].

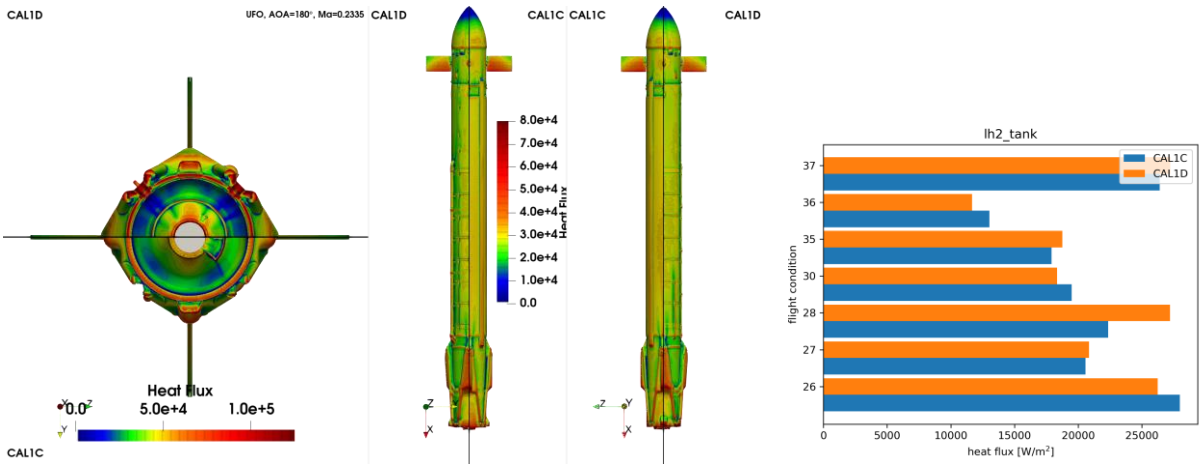

Figure 14: Comparison of aerothermal loads between CAL1C and CAL1D. Left: Visualization of surface heat flux for three different view point of the vehicle for UFO configuration, Ma = 0.7, AoA = 180°. Each view combines half section of CAL1C and CAL1D. Right: Comparison of integral heat flux onto the LH_2 tank for different flight conditions.

A preliminary study of the influence of the geometry evolution on the aerothermal database has been done on the basis of the aerodynamic simulations. Comparisons of heat fluxes between the CAL1C and CAL1D aeroshape are shown in Figure 14 and reveal a good agreement. Noticeable differences in the surface heat flux visualisation on the left are due to the circular struts on the tanks, the additional flange on the aft-bay and the landing leg covers. These features interact with the plume in backward powered flight leading to higher heat fluxes upstream of the features and lower heat fluxes down steam. While the influence of the changes in geometry is visible, it is very localised and not major. This is confirmed by analysing the integral heat flux onto sections of the structure. One of these analyses can be seen in Figure 14 on the right for the LH_2 tank over different flight conditions. The differences are generally low, thus confirming the applicability of the existing CAL1C aerothermal database to the CAL1D Callisto vehicle. A more detailed analysis of the preliminary aerothermal study is being presented in [5] and a dedicated investigation is to follow.

9. Summary and Conclusions

- The mission analysis allowed defining the primary and additional configuration necessary for AEDB to simulate the reference mission (Demo-Flight) as well as the majority of the Test Flights.
- The existing AEDB was extended especially for the simulation of the Test Flight C, this extension considers the fins deployment process.
- The various aspects of model adequacy were discussed, the philosophy of "Delta-Aerodynamics"-Concept was presented.
- The CALLISTO shape evolution and its impact of the aerodynamic and uncertainties was discussed. The developed 'watertight' model of the vehicle CAL1D reflected all the essential details of the considerably more complex aerodynamic shape. This model has been applied for the generation of the aerodynamic meshes for CFD simulations which were used according to proposed "Delta-Aerodynamic"-Concept for comparison with existing AEDB based on CAL1C aeroshape.
- The elastic deformation as result of the aerodynamic loads has not neglectable impact on the fin efficiency.
- Especially the aerothermodynamic aspects play a very important role for a reusable vehicle. The created ATDB allows estimating thermodynamic flux and integrated thermal loads during the reference mission, important data for the design of the thermal protection system.

References

[1] Dumont, E. et. al. (2022) *CALLISTO: A Prototype Paving the Way for Reusable Launch Vehicles in Europe and Japan*. 73rd International Astronautical Congress (IAC), 18–22 September 2022, Paris, France.

DOI: 10.13009/EUCASS2023-510

[2] Klevanski, J., Reimann, B., Krummen, S., Ertl, M., Ecker, T., Riehmer, J., and Dumont, E.. (2022) *Progress in Aerodynamic Studies for CALLISTO - Reusable VTVL Launcher First Stage Demonstrator.* EUCASS 2022, 27 June – 1 July 2022, Lille, France.

[3] Ecker, T., Ertl, M., Klevanski, J., Krummen, S., and Dumont, Etienne (2022) *Aerothermal characterization of the CALLISTO vehicle during descent.* EUCASS 2022, 27 June – 1 July 2022, Lille, France.

[4] Ertl, M., Ecker, T., Klevanski, J., Dumont, E., and Krummen, S. (2022) *Aerothermal analysis of plume interaction with deployed landing legs of the CALLISTO vehicle.* EUCASS 2022, 27 June – 1 July 2022, Lille, France.

[5] Ertl, M., Ecker, T. (2023) *Aerodynamic and aerothermal comparison between the CAL1C and CAL1D geometries for the CALLISTO vehicle.* Aerospace Europe Conference 2023 – 10TH EUCASS – 9TH CEA, 2023.

[6] Riehmer, J., Kapteijn, K., Klevanski, J., Reimann, B., Krummen, S., Gülhan, A., and Dumont, E.. (2022) *Wind Tunnel Experiments of the CALLISTO VTVL Launcher in the TMK and HST Wind Tunnels.* EUCASS 2022, 27 June – 1 July 2022, Lille, France.

[7] Dumont, E. et. al. (2021) *CALLISTO: A Demonstrator for Reusable Launcher Key Technologies.* Transactions of the Japan Society for Aeronautical and Space Sciences, Aerospace Technology Japan, JSASS 19 (1), pp. 106–115, 2021, DOI: 10.2322/tastj.19.106.

[8] Guedron, S. et. al. (2020) *CALLISTO DEMONSTRATOR: Focus on system aspects.* 71st International Astronautical Congress (IAC), 12–14 October 2020, online. URL: https://elib.dlr.de/138808/

[9] Wartemann, V., Konosidou, N., Flock, A., and C. Merrem (2021). *Contribution of numerical and experimental flow simulations to the aerodynamic data base of the DLR reusable flight experiment ReFEx*. Notes on Numerical Fluid Mechanics and Multidisciplinary Design, vol. 151. Springer. DOI: 10.1007/978-3-030-79561-0_14 URL: https://link.springer.com/chapter/10.1007/978-3-030-79561-0_14

[10] Sagliano, M., Macés Hernández, J. A., Fari, S., Heidecker, A.,Schlotterer, M., Woicke, S., Seelbinder, D., Krummen, S., and Dumont, E. (2023) *Unified-Loop Structured H-Infinity Control for Aerodynamic Steering of Reusable Rockets*. Journal of Guidance, Control, and Dynamics, 46(5), 815-837. URL: https://arc.aiaa.org/doi/full/10.2514/1.G007077

[11] Krummen, S., Tummala, P., Wilken, J., Dumont, E., Ertl, M., Ecker, T., Riemer, J., and Klevanski, J. (2023). *Applying Bayesian Inference to Estimate Uncertainties in the Aerodynamic Database of CALLISTO*. 2023 IEEE Aerospace Conference, Big Sky, MT, USA, 2023, pp. 1–18, DOI: 10.1109/AERO55745.2023.10115932. URL: https://ieeexplore.ieee.org/document/10115932

[12] Salvatier, J. and Wiecki, T. V., and Fonnesbeck, C. (2016). *Probabilistic programming in Python using PyMC3*. PeerJ Computer Science, 2:e55. DOI: 10.7717/peerj-cs.55 URL: https://peerj.com/articles/cs-55/

[13] Klevanski, J. and Ecker, T., Riehmer, J. and Reimann, B., Dumont, E., and Chavagnac, C. (2018) *Aerodynamic Studies in Preparation for CALLISTO - Reusable VTVL Launcher First Stage Demonstrator.* 69th International Astronautical Congress (IAC), 1-5 October 2018, Bremen, Germany. URL: https://elib.dlr.de/122062/

[14] Marwege, A., Riehmer, J., Klevanski, J., Gülhan, A., Ecker, T., Reimann, B., and Dumont, E. (2019) *First Wind Tunnel Data of CALLISTO - Reusable VTVL Launcher First Stage Demonstrator.* EUCASS 2019, 1–4 July 2019, Madrid, Spain. URL: https://elib.dlr.de/128629/

[15] Marwege, A., Riehmer, J., Klevanski, J., Gülhan, A. and Dumont, E. (2019) *Wind Tunnel investigations in CALLISTO - Reusable VTVL Launcher First Stage Demonstrator.* 70th International Astronautical Congress (IAC), 21–25 October 2019, Washington D.C., United States. URL: https://elib.dlr.de/132566/

[16] Riehmer, J., Marwege, A., Klevanski, J., Gülhan, A. and Dumont, E. (2019) *Subsonic and Supersonic Ground Experiments for the CALLISTO VTVL Launcher Demonstrator*. International Conference on Flight Vehicles, Aerothermodynamics and Re-entry Missions & Engineering, 30 September – 3 October 2019, Monopoli, Italy. URL: https://elib.dlr.de/137501/

[17] Hofstee, J., Kier, T., Cerulli, C., and Looye, G. (2003) *A Variable, Fully Flexible Dynamic Response Tool for Special Investigations (VARLOADS).* Proceedings of the International Forum on Aeroelasticity and Structural Dynamics, 2003.

[18] Kier, T. M. (2005) *Comparison of Unsteady Aerodynamic Modelling Methodologies with respect to Flight and Loads Analysis.* AIAA Atmospheric Flight Mechanics Conference and Exhibit 2005, San Francisco, CA, United States.

[19] Kier, T., Looye, G., Scharpenberg, M., and Reijerkerk, M. (2007) *Process, methods and tools for flexible aircraft flight dynamics model integration.* International Forum on Aeroelasticity and Structural Dynamics, 2007.

[20] Kier, T. M. (2012) *Aerodynamic Modelling for Integrated Loads Analysis Models.* 3rd Symposium on Simulation of Wing and Nacelle Stall, 2012.

[21] Briese, L. E., Kier, T. M., Petkov, I., Windelberg, J., Heinrich, L., and Krummen, S. (2023) *Advanced Modeling and Dynamic Stability Analysis of the Aerodynamic Control Surfaces of CALLISTO.* AIAA SciTech 2023, 23–27 January 2023, National Harbor, MD, United States. URL: https://arc.aiaa.org/doi/10.2514/6.2023-2405